Bioresource Technology 411 (2024) 131233

Contents lists available at ScienceDirect

Bioresource Technology

journal homepage: www.elsevier.com/locate/biortech

Variation of viscoelastic properties of extracellular polymeric substances and their relation to anaerobic granule's mechanical strength in full-scale treatment plants

Chang Gao [a], Mehdi Habibi [b], Tim L.G. Hendrickx [c], Huub H.M. Rijnaarts [a], Hardy Temmink [a], Dainis Sudmalis [a,*]

[a] Department of Environmental Technology, Wageningen University and Research, Bornse Weilanden 9, 6708 WG Wageningen, the Netherlands
[b] Laboratory of Physics and Physical Chemistry of Foods, Wageningen University and Research, Bornse Weilanden 9, Wageningen 6708 WG, the Netherlands
[c] Paques Technology B.V., T. de Boerstraat 24, Balk 8561 EL, the Netherlands

HIGHLIGHTS

- Granules from nine anaerobic WWTPs are characterized.
- Relations between granule strength and the extracted EPS are quantitatively studied.
- Gel softening rates can well explain granule's shear strength.
- PN components in the EPS can determine their nonlinear behavior under shear strain.

GRAPHICAL ABSTRACT

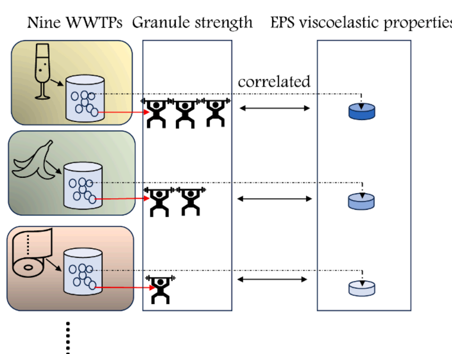

ARTICLE INFO

Keywords:
Anaerobic granules
Extracellular polymeric substances
Mechanical strength
Rheology

ABSTRACT

Extracellular polymeric substances (EPS) are considered to play a pivotal role in shaping granules' physical properties. In this contribution, we characterized the viscoelastic properties of EPS from granules of 9 full-scale industrial anaerobic reactors; and quantitatively investigated whether these properties correlate with granules' resistance to compression ($E_{granule}$) and shear strength ($S_{granule}$). Most granules with a higher shear strength, also exhibited a stronger resistance to compression ($r = 0.96$, $p = 0.002$), except those granules that contained relatively more proteins in their EPS. Interestingly, these granules were also the most resistant to shear stress ($S_{granule} \geq 110 \pm 40$ h). Furthermore, the EPS hydrogels of these granules had slower softening rates ($\kappa < 0.9$) compared to the others (κ ranged between 0.95 and 1.20), indicating stronger gels were formed. These findings suggest that the EPS hydrogel softening rate could be a key parameter to explain granule's shear strength.

* Corresponding author.
E-mail address: dainis.sudmalis@wur.nl (D. Sudmalis).

https://doi.org/10.1016/j.biortech.2024.131233
Received 14 July 2024; Accepted 5 August 2024
Available online 6 August 2024

1. Introduction

Anaerobic wastewater treatment is a widely applied process to purify streams highly polluted with organics (Horan, et al., 2018). Some anaerobic reactors, such as upflow anaerobic sludge blanket (UASB) and expanded granular sludge bed (EGSB) can treat wastewaters in a reactor with a high volumetric loading rate by effectively decoupling hydraulic residence time from sludge residence time (van Lier, 2008). This is ensured through the formation of dense, well-settling, physically strong, and active microbial granules (McHugh et al., 2003). Hence, their formation and stability are crucial for well-functioning high-rate reactors.

It is accepted that, amongst others, extracellular polymeric substances (EPS) play an important role in the anaerobic granulation process and biofilm formation in general (Dubé and Guiot, 2019). The EPS are produced by microbial communities within granules and consist of a variety of molecules, such as humic acids, proteins, glycoproteins, and polysaccharides (Seviour et al., 2009a). Typically, proteins (PN) account for the major proportion of EPS in anaerobic granules followed by polysaccharides (PS) (Dubé and Guiot, 2019). Some work suggests that anaerobic granules are stronger when the EPS contain more PS (Quarmby & Forster, 1995; Hudayah et al., 2019). This might be due to their ability to form strong EPS hydrogels (Seviour et al., 2009b). Particularly, the alginate-like EPS (ALE, mostly abundant in PS) were found to be the key components that determine the gelling capacity of exopolymers in aerobic granules (Lin et al., 2008). Since they form hydrogels, the viscoelastic properties of EPS are generally considered to be related to the stability of granules (Campo et al., 2022; Seviour et al., 2009a).

To date, most work focused on comparing the viscoelastic properties of the extracted EPS from aerobic granules and non-granular sludge (e.g. flocculant sludge) (Seviour et al., 2009b; Schambeck et al., 2020). It was shown that the EPS extracted from aerobic granular sludge can form strong EPS gels at pH <9, while this was not observed for those extracted from flocculant sludge. Interestingly, the PS concentrate of the granular EPS had a similar gel stiffness as that of the overall EPS (Seviour et al., 2009b). Other research also found hydrogels were stiffer with the ALE extracted from aerobic granules compared to that from flocculant sludge (Schambeck et al., 2020). Additionally, some studies observed a decreasing granules' stiffness after EPS extraction (Li et al., 2020; Ma et al., 2014). The results of these studies all indicate a potential link between the viscoelastic properties of EPS, especially their PS fraction, and aerobic granule's physical properties.

However, the EPS of anaerobic granules mainly consist of proteins (PN) and typically only contain a minor fraction of polysaccharides (Dubé and Guiot, 2019; Ding et al., 2015). It is expected that besides the PS fraction in EPS, the physics of the granules is also affected by the collective arrangement of various molecules that build up these structures (Lee et al., 2010). For instance, Shi and Liu (2021) found that the β-sheet structures in PN were also significantly involved in the stability of aerobic granules. A simultaneous decrease of the β-sheets abundance and granule's size was observed in their research. This agrees with Flemming and Wingender (2010) who reported that PN in general could contribute to the stability of biofilms due to their adhesive properties.

It is worth noting that most studies have linked EPS viscoelastic properties to granule "stability", encompassing aspects such as granule diameter, granule viscoelastic properties, or granule resistance to digestion (Lin et al., 2008; Seviour et al., 2009a; Guo et al., 2020). However, no research has clearly investigated the correlation between granules' mechanical strength and EPS viscoelastic properties. In high rate anaerobic reactors, granules experience high shear forces due to biogas production and liquid flow (Liu and Tay, 2002). Therefore, it is particularly crucial to investigate the impact of EPS viscoelastic properties on granules' strength in high rate anaerobic reactors.

As outlined above, most of the work on EPS viscoelastic properties and their relation to granule properties was conducted in the closely related field of aerobic granular sludge (Pagliaccia et al., 2022; Seviour et al., 2009a), and without the purpose of sampling a broad range of granules. To the best of the authors' knowledge, there is no work available that investigates relationships between the strength of granules in full-scale industrial anaerobic reactors and hydrogels formed from their extracted EPS. Thus, in this contribution, we aim to extend the understanding of such relations from aerobic to the anaerobic granular sludge field. To that end, granules and their extracted EPS from 9 full-scale anaerobic reactors treating various wastewaters were investigated. We quantitatively analysed the composition and viscoelastic properties of EPS hydrogels and related these to the mechanical strength of the granules. Our findings highlight the crucial role of protein in determining EPS non-linear behaviour and introduce a previously overlooked parameter: the softening rate of hydrogels, which can effectively explain the shear strength of granules.

2. Materials and Methods

2.1. Source of granules

The microbial communities within granules, and EPS composition in return, depend on wastewater composition (Batstone and Keller, 2001; Gagliano et al., 2020). Hence, the anaerobic granules were sampled from 9 full-scale applications treating a variety of wastewaters and stored at 4 °C before analysis. The wastewater origin, reactor type, and reactor operational parameters of each location are summarized in Table 1, where the full-scale reactors are listed in the order of increasing up-flow velocities.

To exclude flocs and specifically select granules for further strength and EPS analysis, the various size fractions of the sludge were first analysed on a macroscope (Nikon SMZ800, Japan), equipped with a CMEX-5 PRO USB 3.0 camera. The image analysis was performed with Image Focus Alpha software (data not shown). As a result, only particles with a diameter larger than 0.5 mm were considered granules, and they were obtained by sieving the sludge through a 0.5 mm mesh. The morphology of the granules grown on various wastewaters is depicted in **Supplementary material**.

2.2. Characterization of granule's strength

Granules in reactors are being exposed to shear stress resulting from fluid motion, and can also experience deformation stress from collisions among granules and of granules to reactor walls (Liu and Tay, 2002; Zhao et al., 2022). Hence, the characterization of both shear strength and compression strength is important to indicate granules' physical resilience to forces exerted in various hydrodynamic regimes and reactor types.

2.2.1. Shear strength

Theory. The shear strength of the granules can be determined by exposing granules to shear and collecting abraded fines over time. The shear strength of the granules can then be characterized as $S_{granule}$ (in h) according to de Graaff et al. (2020):

$$\frac{dX_F}{dt} = K \times (X_0 - X_F) \tag{1}$$

$$X_F = X_0 - X_0 \times e^{-K \times t} \tag{2}$$

$$S_{granule} = 1 / K \tag{3}$$

where X_F – is the cumulative production of fines (in gTS) within t hours, X_0 – is the dry weight of granules at $t = 0$ (in gTS), K – is the abrasion coefficient (in h^{-1}), and $S_{granule}$ is the shear strength of the granules (in h). The X_F and X_0 were determined according to Standard Methods, 2540 (APHA, 1999).

Experimental approach. The shear strength was determined by

Table 1
Source of granules and wastewater treatment plant characteristics.

Sample (abbreviation)	Reactor Type[a]	Industry for which wastewater is treated	Nutrient dosing	Temperature °C	Effluent VFA[b] mmol/L	Effluent NH_4^+ mg N/L	NH_4^+/VFA mg N/mg VFA	v_{up}^c m/h
P	UASB	Potato industry		32	2.1–3.8	260–280	1.5	<1
RP-1	EGSB	Recycled paper	N&P dosing[e]	36 (33–39)	3.0 (1.4–7.6)	7.0 (3.5–12)	0.04	3.6 (3.2–4.4)
RP-2	EGSB	Recycled paper	N&P dosing	36 (33–39)	8.5 (0.6–20)	48 (0.3–92)	0.09	3.6 (3.2–4.4)
PM	UASB	Papermill		35	0.67–0.83	2–5	0.08	5.4
KW	ICX	Kitchen waste, excluding FOG[d]		31 (28–33)	0.5–5	410 (350–480)	2.5	6.4 (4.7–7.9)
RP-3	ICX	Recycled paper	N&P dosing	37 (32–39)	5.6 (1–22)	24 (0.2–150)	0.07	6.8 (5.7–8.0)
SD	ICX	Soft drink wastewater		36 (35–37)	1 (0–2)	7.4 (6.1–8.3)	0.12	8 (4–13)
RC	IC	Rendering Condensate	N&P dosing	34 (27–37)	9 (3–23)	1420 (800–2400)	2.6	~ 8
T	IC	Tannery wastewater, high salinity		31(30–35)	2.4	550	3.8	15

Note: a) UASB – upflow anaerobic sludge blanket; EGSB – expanded granular sludge bed; IC – internal circulation reactor; ICX – internal circulation experience reactor. The reactors were ordered by the mixing intensity from low to high. b) VFA – volatile fatty acids. c) v_{up} – superficial upflow velocity. d) FOG – Fats, oils, and grease. e) N&P – nitrogen and phosphorus. The values shown in the table are averages.

exposing granules to shear in a bubble column according to Pereboom (1997). In short, 10 g of granules with a known dry weight of X_0 was inserted into a bubble column (D=46 mm, H=305 mm). The column was filled with tap water and sparged with nitrogen gas for approximately 30 min before granule addition. Subsequently, the granules were exposed to high shear by sparging the column with nitrogen gas at a superficial velocity of 61 m/h, which was much higher than typical in practice at full scale (2 ~ 3 $m^3/m^2 \cdot h$) (Lier, 2015). During the shear experiments, the generated fines were collected once an hour for five subsequent hours and their dry weight (X_F) was measured. The "fines" were defined here as particles smaller than 0.5 mm, and $S_{granule}$ was determined by fitting Equation [2] and [3] to the experimental data via an error minimization routine in Microsoft Excel, *Version 2208*. All experiments were performed in duplicate.

2.2.2. Compression strength and elastic modulus

Theory. The compression strength ($E_{granule}$) can be determined by exerting external force on a granule to measure the deformation, and using Equation [4] (Javanmardi et al., 2021):

$$F(x) = \frac{2E_{granule}\sqrt{R}}{3(1-\nu^2)}x^{3/2} \quad (4)$$

where $E_{granule}$ – is the elastic modulus of a granule (in Pa), R – is the equivalent radius of the granule (in m), ν – is the Poisson's ratio (which varies between 0.35 and 0.5 for hydrogel materials, such as granules and biofilms (Javanmardi et al., 2021)), x – is the compaction displacement (in m), F – is the compression force (in N). Granules were approximated as perfect spheres.

Experimental approach. The $E_{granule}$ was measured in a tensile test machine (Stable Micro Systems Texture Analyser TA – TX plus, UK) with an SMS P/20 probe. The compression speed was set to 0.1 mm/s with a target strain of 80 %. During the compression process, the compression force was continuously measured as a function of compaction displacement x. The $E_{granule}$ was calculated by fitting the experimental data to the Hertz model, as shown in Equation [4] (Javanmardi et al., 2021). To calculate the equivalent radius of various granules, the projected cross-sectional area A (in m^2) of the individual granule was measured first via macroscopic imaging, and from that an equivalent radius (R, in m) was calculated. The analysis was performed in triplicate and the details of the calculation are explained by analysing data in the **Supplementary material** with granules treating potato wastewater (P) as an example.

2.3. Characterization of EPS

2.3.1. Extraction of EPS and quantification of polysaccharide and protein content

The EPS were extracted from granules by a slightly modified "alkaline heat extraction" method according to Felz et al. (2016). The modifications included the use of 15 g of granules instead of 3 g to extract more EPS for the mechanical characterization of EPS hydrogels formed from the extracted EPS. The extraction volume was increased to 250 ml accordingly. These modifications did not result in measurable changes in EPS extraction yield compared to the original protocol (data not shown).

The PS content of EPS was quantified according to DuBois et al. (1956), using a phenol–sulphuric acid method with glucose as equivalents. The PN content of EPS was quantified according to Williams et al. (1987). The total nitrogen concentration in the EPS was measured by Hach Lange Kits (LCK338), and the PN concentration was calculated by multiplying the total nitrogen concentration with a factor of 6.25.

2.3.2. Fourier transform infrared spectroscopy (FTIR)

The extracted EPS were freeze-dried in a 2.5 Liter Benchtop Freeze Dryer (Labconco, the US) at −80 °C and 0.001 mbar. The functional groups of the lyophilized EPS were determined by a compact FTIR (ALPHA II) coupled with platinum Attenuated Total Reflectance (ATR) (Bruker, the US). The secondary structures of proteins were analysed by the software OPUS 8.1 at a scanning range from 1700 to 1400 cm^{-1} and a spectral resolution of 2 cm^{-1}.

2.3.3. Determination of gelling concentration

To determine the concentration at which EPS form a hydrogel, solutions with different concentrations of lyophilized EPS were dialyzed in 10 g/L $CaCl_2$ solution for 24 h at room temperature (Felz et al., 2020). The minimal EPS concentration for gelling was found to be equal to or higher than 150 g/L (data not shown); above that concentration, stiff hydrogels could be formed with EPS of all granules.

2.3.4. Viscoelastic properties of EPS

Theory. The matrix of anaerobic granules is composed of bacteria and archaea bound together by EPS which functions as a hydrogel. By extracting the EPS from granules and characterizing their viscoelastic properties, these can be related to the granule's strength and EPS chemical parameters. EPS hydrogels are viscoelastic materials, where both elastic and viscous properties can contribute to their behaviour upon exposure to stresses (Ayol et al., 2006; Ni et al., 2015). These properties can be assessed in a rheometer by shear oscillation with a constant (varied) angular frequency (ω) and shear strain (γ), where the elasticity and viscose property is represented by the storage modulus (G') and loss modulus (G''), respectively. The oscillation tests are generally divided into three stages: time sweep, frequency sweep, and amplitude sweep. In a time sweep at low angular frequency, a small shear strain was applied to probe the samples and track the change of their viscoelastic properties during gelation. In a frequency sweep, the viscoelastic behaviour of EPS gels can be confirmed at fixed shear strain by stepwise decreasing angular frequency through the power-law scaling relationships $G' \sim \omega^{\alpha}$ and $G'' \sim \omega^{\beta}$ (Jaishankar and McKinley, 2013). During an amplitude sweep, the stiffness of EPS gels and their nonlinear behaviour can be determined by a stepwise increased shear strain at a fixed angular frequency. First, regions where *G'* and *G"* are more or less constant indicate the linear viscoelastic regime (LVE) (Farno et al., 2016). The stiffness of the EPS gel can be represented by the absolute complex modulus (*G**) at LVE, which was calculated from the *G'* and *G"* by Equation [5] (Willits and Skornia, 2004).

$$G^* = \sqrt{G'^2 + G''^2} \quad (5)$$

As shear strain (γ) is further increased, a critical strain (Strain I) is reached where the moduli of hydrogels start to decrease, often denoted as strain softening ($G^* \sim \gamma^{-\kappa}$, where κ is the softening rate). At strain I, G^* of the EPS gel is decreased to 95 % of its initial linear-regime value, indicating the onset of nonlinear viscoelastic behaviour, i.e. gel structure breakage and increasing deformation (Giménez-Ribes et al., 2023). Further increase of the shear strain results in a faster decrease of *G'* than *G"*. At the point where *G'* and *G"* intersect (Strain II), the system transitions from solid-like ($G'' < G'$) to liquid-like ($G'' > G'$) structure (Ayol et al., 2006).

Experimental approach. The viscoelastic properties of the EPS hydrogels formed with EPS extracted from different granules were determined in a series of shear oscillation tests. First, the lyophilized EPS were dissolved in 10 g/L $CaCl_2$ solution to form EPS solution of 150 g/L. Further, the EPS solution was transferred to a rheometer (Anton Paar MCR 502, with a plate-plate geometry PP25/SS, Austria) to allow the EPS hydrogels form *in situ*. The angular frequency (ω) and shear strain (γ) during each stage of the oscillation test are summarized in Table 2.

2.4. Statistical analysis

Statistical analysis was carried out by Origin Pro 2023b to assess the relationship between the physical properties of anaerobic granules and their extracted EPS. Correlation analysis was carried out using Pearson's correlation *r*, and a strong positive correlation can be indicated with $r > 0.60$ (Liu, 2021). ANOVA was used for the significance test at the 95 % confidence level (Thapa, 2019).

3. Results and discussion

3.1. Physical and chemical properties of the granules

Amount and Composition of EPS. Fig. 1 summarizes the EPS content and corresponding protein (PN) to polysaccharide (PS) ratios for granules grown on various wastewater types and hydrodynamic regimes. Granules from papermill (PM) contained the highest EPS quantity (70 ± 1.2 mg EPS-VS/g WW), while those from rendering condensate (RC) contained the lowest EPS quantity (28 ± 0.5 mg EPS-VS/g WW). Most granules showed similar compositions in their EPS with PN/PS ratios varying from 5.8 to 6.9, except granules from potato wastewater (P), kitchen waste (KW), and soft drink wastewater (SD). These granules had the highest PN/PS ratios (PN/PS ratios ≥ 8) in their EPS. The EPS content and composition measured in our study are comparable with that reported by D'Abzac et al. (2010).

Granule Strength. Although varying in colour and shape, the granules from various WWTPs appeared dense and well-developed. Nevertheless, distinctions on the shear strength of granules ($S_{granule}$) and their resistance to compression ($E_{granule}$) were found as illustrated in Fig. 2-**a** and Fig. 2-**b**. The error bars shown in Fig. 2-**b** are higher than the

Table 2
Operational parameters for the oscillation test in each stage.

	Angular frequency (rad/s)	Shear Strain (%)
Time Sweep	1	0.01
Frequency Sweep	100 to 0.1	0.1
Amplitude Sweep	1	0.01 to 1000

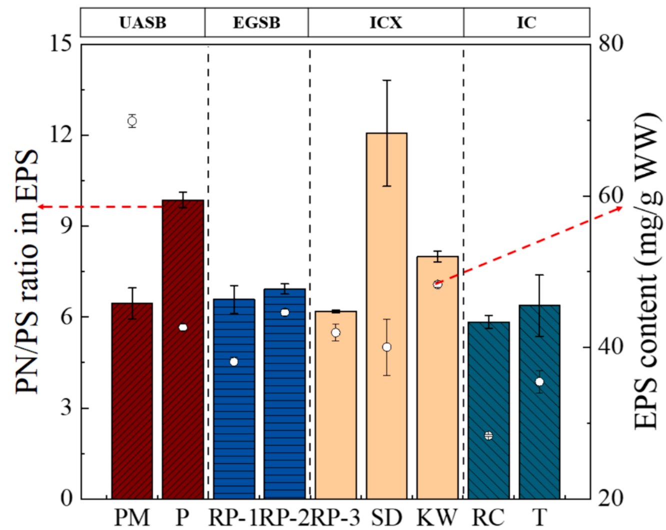

Fig. 1. EPS content and PN/PS ratios in the EPS extracted from granules of different anaerobic WWTPs. The columns indicate the PN/PS ratios in the EPS. The open circles indicate the amount of the extracted EPS volatile solids (organic fraction of EPS) normalized per g of wet weight (WW) of granules. The errors are standard deviations of triplicate measurements. PM-papermill, P-potato, RP-recycled paper, SD-soft drink, KW-kitchen waste, RC- rendering condensate, and T-tannery.

deviation of the $E_{granule}$ calculated with different Poisson's ratios (0.35 and 0.5, data not shown), indicating a neglectable influence caused by Poisson's ratio on $E_{granule}$ calculation.

The granules with the highest shear strength developed in the soft drink (SD), potato (P), and kitchen waste (KW) wastewater treatment plants ($S_{granule,\ SD}$=130 ± 13h; $S_{granule,\ P}$=110 ± 40h; $S_{granule,\ KW}$=110 ± 10*h*) (Fig. 2-**a**), while the weakest granules were found in recycled paper wastewater (RP-1) ($S_{granule}$ = 15 ± 3.2 h). This is consistent with the observation of Forster and Quarmby (1995), where the granules grown on potato wastewater exhibited the highest shear strength compared to those treating other wastewaters (e.g. paper, wheat starch, and distillery). Compared to the granule's shear strength, the values for uni-axial compression strength are insignificantly different for all the granule samples of the different wastewaters, considering the measurement uncertainty (Fig. 2-**b**). Interestingly, when grouping granules based on the reactor type from which they were sampled (UASB, etc.), we found that most granules growing in reactors with higher effluent NH_4^+/VFA ratios were more resistant to shear (Fig. 2-**a**), except the granules from ICX reactors.

In Fig. 3, $S_{granule}$ versus $E_{granule}$ is shown. It becomes clear, that the sampled granules fall into two distinct groups: i) with $S_{granule}$ below 60 h and; ii) with $S_{granule}$ above 100 h. Furthermore, it seems that in full-scale reactors granules with excellent shear strength can develop irrespective of reactor configuration (Fig. 2-**a** and Fig. 3). The granules exhibiting the higher shear strength were also more resistant to compression (Fig. 3), especially when separating based on their shear strength, as explained above. The trend between $S_{granule}$ and $E_{granule}$ among samples SD, KW, and P shows strong positive correlation with $r = 0.90$. For the remaining samples this correlation is also strongly positive with $r = 0.96$. Thus, our study clearly demonstrates strong correlation between $S_{granule}$ and $E_{granule}$.

Interestingly, the granules grown on different organic substrates fall into two distinct groups. The first group includes granules from soft drink (SD), kitchen waste (KW), and potato industry (P) wastewater. The EPS of these granules contained higher PN/PS ratios and granules were more resistant to shear. All remaining granules belong to the second group. The EPS of these granules had lower PN/PS ratios in their EPS and the granules were less resistant to shear stress (Fig. 1, Fig. 3).

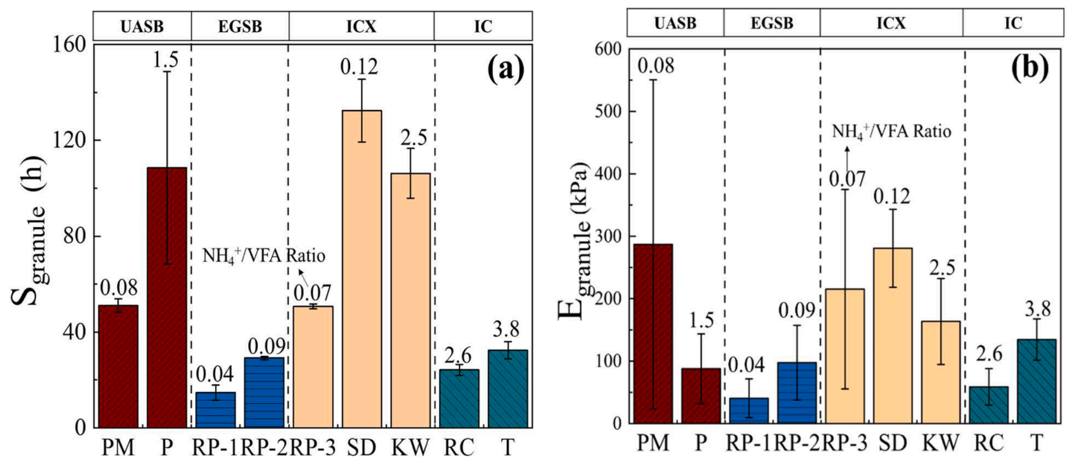

Fig. 2. (a) Shear strength ($S_{granule}$) of the granules from different anaerobic WWTPs. The error bars show the absolute deviation of duplicate measurements. (b) Elastic moduli of the granules ($E_{granule}$) from different anaerobic reactors. The error bars show the standard deviation of triplicate measurements. The NH_4^+/VFA ratios in effluent (Table 1) are ordered from low to high for each reactor type, and the values are shown above the columns. PM-papermill, P-potato, RP-recycled paper, SD-soft drink, KW-kitchen waste, RC- rendering condensate, and T-tannery.

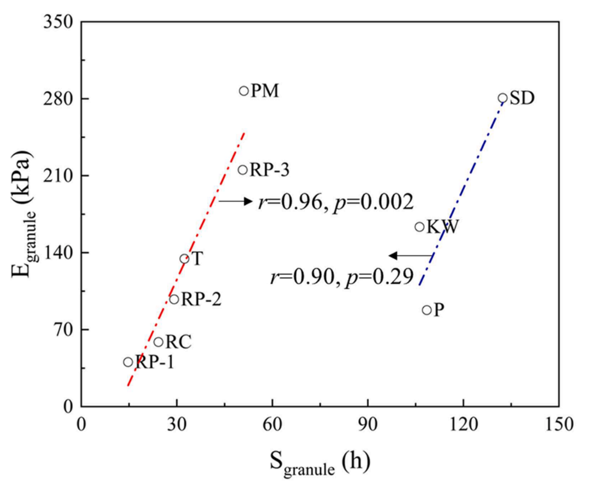

Fig. 3. Relationship between granule's shear strength ($S_{granule}$) and resistance to compression ($E_{granule}$). The data points represent average values and are divided into two groups based on their shear strength. The dashed lines are trend lines of linear correlations in each group to guide the reader's eye. PM-papermill, P-potato, RP-recycled paper, SD-soft drink, KW-kitchen waste, RC-rendering condensate, and T-tannery.

3.2. The viscoelastic behaviour of EPS gels

To investigate the contribution of EPS gels to the overall granule's mechanical strength, and explain the different behaviour of soft drink, kitchen waste, and potato granules (SD, KW, and P in Fig. 3), the EPS hydrogel viscoelastic properties from granules at various WWTPs were analysed. In general, the EPS gels' stiffness (G^*) and softening rate (κ) varied broadly among different samples ($G^* \in$ [1.3 kPa, 33 kPa], $\kappa \in$ [0.65, 1.2] in Table 3). This resembles the broad variation of granule's shear and compression strength (Fig. 2).

The evolution of storage (G') and loss moduli (G'') during the gelling process (time sweep) are illustrated in Fig. 4-**a** with the EPS extracted from granules growing on papermill (PM) and potato wastewater (P) as an example. The results for the EPS gels of all other classes of granules showed the same behaviour (data not shown). As shown in Fig. 4-**a**, both moduli increased in time, corresponding to the proceeding of gel formation and increasing bond formation between EPS molecules. Finally, after about 22 h the reaction approached equilibrium, as shown by plateau values of G' and G'' with time. In all samples the G' was larger than G'' (Fig. 4-**a**), indicating a solid-like behaviour of the gel (Ni et al., 2015; Wang et al., 2020).

To confirm that indeed viscoelastic EPS gels were formed they were further investigated in a frequency sweep, where G' and G'' were analysed as a function of angular frequency as in Fig. 4-**b** with PM and P as an example. The results of all hydrogels are shown in **Supplementary material**. For all the samples, G' and G'' remained almost parallel with each other in the log–log plots by increasing frequency. When analysing

Table 3
Comparison of the linear and nonlinear response of EPS gels during amplitude sweep (color).

	RC	RP-3	T	PM	RP-1	RP-2	KW	P	SD
	Rendering condensate	Recycled paper	Tannery	Papermill	Recycled paper	Recycled paper	Kitchen waste	Potato	Soft drink
PN/PS ratios	5.82	6.19	6.43	6.44	6.55	6.93	7.99	9.85	11.79
G' (kPa)	9.53	7.78	13.49	30.95	1.04	1.24	1.07	1.72	8.22
G^* (kPa)	10.46	8.14	14.46	33.16	1.89	1.28	1.28	1.81	8.57
Strain I (%)	0.79	0.53	0.36	0.36	0.24	0.53	1.75	0.79	0.36
Strain II (%)	19.79	27.43	9.33	12.25	19.14	23.18	27.05	14.76	39.66
κ	1.07	1.17	0.95	1.17	1.20	1.05	0.70	0.65	0.89

Note: The samples in the table are ordered according to the PN/PS ratios from low to high. 1) G* was measured at LVE. The samples in dark green color indicate the ones with higher gel stiffness ($G^* > 8$ kPa), while the ones in light green color have lower gel stiffness ($G^* < 2$ kPa). 2) Softening rate (κ) was calculated by fitting the experimental data to the model ($G^* \sim \gamma^{-\kappa}$) in the shear strain ($\gamma$) ranging from 8.6 % to 100 %.

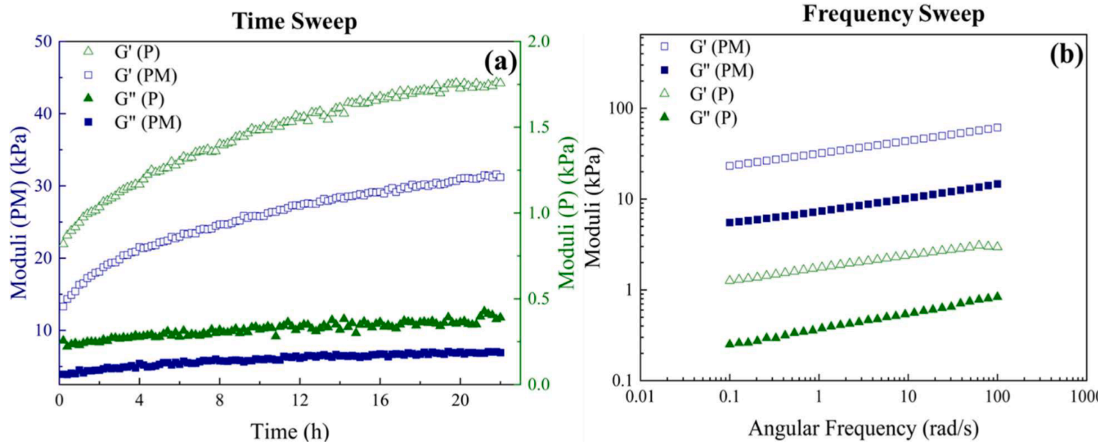

Fig. 4. (a) G' and G" of EPS gels formed from granules grown on papermill wastewater (PM on the left axis) and potato wastewater (P on the right axis) during the time sweep. (b) G' and G" of EPS gels formed from granules PM and P during the frequency sweep.

the power-law relation between moduli and frequency ($G' \sim \omega^{\alpha}$, $G" \sim \omega^{\beta}$), the values of the exponents were found to be rather low, namely $\alpha \in [0.09, 0.15]$ and $\beta \in [0.11, 0.19]$ (**Supplementary material**). This is comparable with the EPS gels formed from aerobic granules (dry matter content varying from 2.1 % to 4.2 %) with α and β around 0.5 (Schambeck et al., 2020), and that of activated sludge where $\alpha = 0.1$, $\beta \in [0.1, 0.2]$ (Farno et al., 2016).

To further investigate the nonlinear rheological responses of EPS hydrogels under shear, the amplitude sweep test was performed. The complete set of the results is depicted in **Supplementary material** and again PM and P are shown as examples (Fig. 5-**a**). The G' and $G"$ of both EPS gels were independent of shear strain at LVE regime. Then, the moduli started to decrease at Strain I (0.3 %), and a cross-over point of G' and $G"$ was observed at Strain II (13 %) where the hydrogel transitioned to a liquid-like behaviour (Fig. 5-**a**). Similarly, previous research showed that Strain I and Strain II were around 0.4 % and 10 % for the EPS gels formed from aerobic granular sludge (Campo et al., 2022).

Additionally, the variation of G^* during the amplitude sweep is illustrated in Fig. 5-**b** with PM and P as an example to illustrate the softening rate (κ). Stronger gel strength of P was indicated in Fig. 5-**b** by a slower decrease of G^* (lower κ) compared to PM. The key parameters obtained during the amplitude sweep for all EPS gels are summarized in Table 3, which clearly shows that distinct hydrogel properties are obtained from various granules, even when similar wastewaters are treated. The stiffness and strength of EPS gels measured in our study are similar to that extracted from aerobic granular sludge grown on abattoir wastewater (G^* around 10 kPa, κ around 1 at $\omega = 5$ rad/s) (Seviour et al., 2009b).

Among all the samples, RP-1, RP-2, P, and KW were relatively brittle, with G^* lower than 2 kPa in the LVE region. In contrast, the G^* for the other samples were much higher, varying from 8.1 kPa to 33 kPa. Upon increasing shear strain, the onset of nonlinear behaviour (Strain I) and liquid-like behaviour (Strain II) varied broadly across the different hydrogels (Strain I from 0.24 % in RP-1 to 1.8 % in KW, Strain II from 9.3 % in T to 40 % in SD), indicating the different endurable shear strain for various EPS gels.

Typically, the stiffness of EPS gels is compared by measuring the G' at LVE without destroying the gel structure (Schambeck et al., 2020; Wang et al., 2020). This way of comparison led to the conclusion that PS are the main components in determining EPS gel's stiffness (Seviour et al., 2009b). From this point of view, our results are consistent with the previous studies, and EPS with average PN/PS ratios lower than 6.5 (PM, RP3, T, and RC) formed stiffer hydrogels with G' higher than 7 kPa at LVE. The same conclusion can be made when taking the viscose properties measured as $G"$ into consideration. We show that lower PN/PS ratios resulted in higher gel stiffness, measured as G^*.

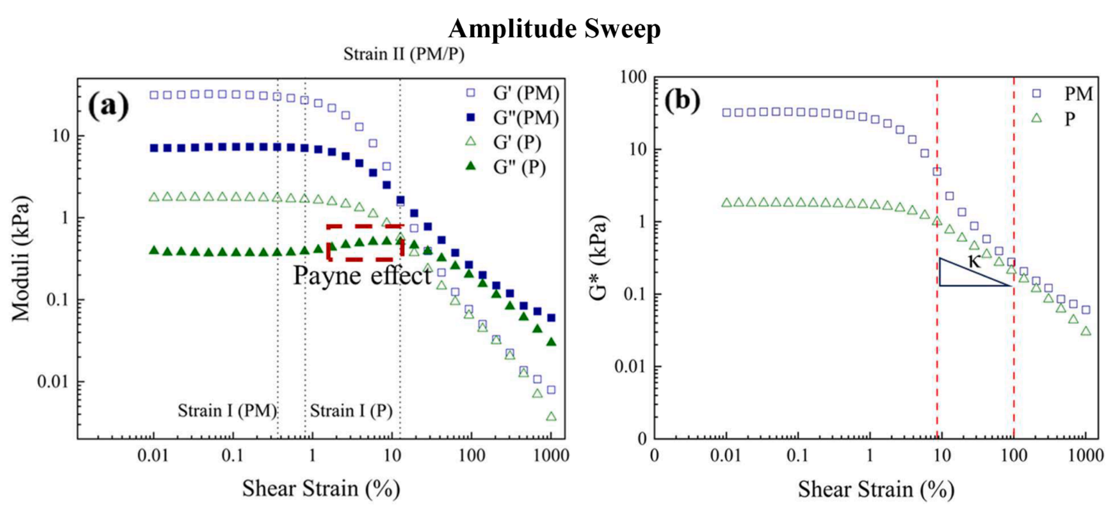

Fig. 5. (a) G' and G" for the EPS hydrogels PM (papermill) and P (potato) during the amplitude sweep. The Strain I is the threshold of nonlinear behaviour determined by the strain where a 5% decrease is observed in G*, and Strain II is the strain where G' and G" intersect with each other and the gel transitions to liquid-like behaviour. (b) G* of the EPS hydrogels (PM and P) during the amplitude sweep. κ is the softening rate, which is represented by the slope of G* at shear strain (γ) ranging from 8.6% to 100%.

In addition to the G* measured at LVE, EPS gel's nonlinear behaviour could also significantly influence granules' mechanical strength, particularly their shear strength. This is because granules are abraded during exposure to high shear forces (de Graaff et al., 2020), which indicates an irreversible breakage of the polymer network in the granules. As the strain of gel during the amplitude sweep increased at a constant speed, the rate at which EPS hydrogels break is determined by the softening rate κ, i.e., the lower the κ, the slower the breakage. Notably, the EPS hydrogels of granules SD, KW, and P which had the highest average PN/PS ratios (Fig. 1) had the lowest softening rate ($\kappa < 0.9$) (Table 3). Thus, these EPS hydrogels are less vulnerable to structural breakage at shear strains beyond their yield point.

Interestingly, KW and P which had the lower κ exhibited overshoots in the curves of G" during the amplitude sweep (Fig. 5**-a** and **Supplementary material)**. This phenomenon is known as the "Payne effect", and is attributed to the reorganization of bonds which create more energy dissipation (Ma et al., 2014). The "Payne effect" was also observed in the 2D gel formed from whey protein-escin mixtures (Giménez-Ribes et al., 2023) and EPS of aerobic granular sludge (Ma et al., 2014). It is important to note that the granules SD, KW, and P with EPS hydrogels less susceptible to breakage were also the most resistant to shear stress (Fig. 2**-a**, Fig. 3). Besides, they also had higher PN/PS ratios in their EPS. Thus, proteins seem to be crucial in ensuring EPS gel's strength in nonlinear behaviour regime and therefore also anaerobic granule's strength.

The viscoelastic properties of EPS gels are associated with their composition (Wang et al., 2005). The PN components in the EPS can build up cross-links by hydrogen bonding, covalent disulfide bonding, ionic and hydrophobic interactions, and Van der Waals forces (Zayas, 1997; Sheng et al., 2010). Especially at high protein concentrations, the intermolecular contact between different protein molecules is enhanced and more crosslinks are created. The number of such crosslinks was reported to be closely related to the stiffness of pure protein hydrogels in the field of food technology (Zayas, 1997). On the other hand, the PS components in the EPS can build up an elastic hydrogel structure with Ca^{2+} by forming mono-complexes and egg-box dimers (Pagliaccia et al., 2022). Thus, the PS are also considered to be highly related to the post-gelling stiffness and elasticity of EPS gels (Ding et al., 2015; Campo et al., 2022).

In our study, EPS with similar PN/PS ratios had a broad range of G* and κ (Table 3). Thus, not only the PN/PS ratio but also the type of sugars and proteins involved in the gelation must play a role. Indeed, through analysing the secondary structure of the proteins in the EPS, we found that the EPS that formed the strongest EPS hydrogels (SD, KW, and P) contained proteins with higher β-sheets abundance compared to the weaker counterparts (**Fig. S4**). This could be related to the fact that β-sheet structures require a larger applied force to rupture them when normalized to each hydrogen bond compared to α-helices (DeBenedictis and Keten, 2019). Similarly, the viscoelastic properties of PS (e.g. alginate) rely on the ratio of mannuronic acids blocks (M) and guluronic acids blocks (G). Stiffer gels can be formed with an M/G ratio is less than 1, while an enhancement of gel strength was observed when M/G ratio is higher than 1 (Sarkis, 2023). Thus, the specific structure of PN and PS is essential to be investigated in the future studies on EPS viscoelastic properties.

3.3. Do quantity and viscoelastic properties of EPS gels explain the physics of granules?

The scientific consensus is that the EPS lend some physical properties to granular sludge (Felz et al., 2016; Lin et al., 2008). We put this to a test and investigated the relationships between the strength of anaerobic granules and the viscoelastic properties of their EPS hydrogels. As mentioned above, granules SD, KW, and P demonstrated inconsistent behaviour with the other samples, as their EPS had higher PN/PS ratios, lower EPS gel softening rate, and granules themselves were more resistant to shear. Thus, the 9 samples from different anaerobic WWTPs were divided into two groups for further correlation analysis. Namely granules SD, KW, and P with EPS PN/PS ratios higher than 8; and others with PN/PS ratios lower than 7.

3.3.1. The correlation between EPS quantity and granule's mechanical strength

Interestingly, the quantity of EPS negatively correlated with the shear strength and the elastic modulus in granules SD, KW, and P which were generally more resistant to shear, and originated from food related applications. On the other hand, the correlations were positive in the other group (Fig. 6**-a**, **b)**. The linear relation between EPS quantity and granule's shear strength ($S_{granule}$) and granule's resistance to compression ($E_{granule}$) is shown in Fig. 6**-a** and Fig. 6**-b**, respectively. Both $E_{granule}$ and $S_{granule}$ showed strong correlations with EPS content ($r > 0.60$), but with varying significance at the 95 % confidence level in all cases. It is worth noting though that the essentiality of p-value should not be overestimated (Amrhein et al., 2019), and the relatively higher p-value (>0.05) can be addressed in the follow-up studies by including granules from more full-scale applications in the analysis. Despite the higher p-values, our study presents clear trends between EPS content and granule's physical strength. Interestingly, the trends were opposite among two groups of granules: the higher EPS content weakened the stronger granules (e.g. SD, KW, and P, κ < 0.9), while granule's strength was enhanced by higher EPS content for the other weaker granules. This explains the inconsistent trends observed between EPS content and granule's strength in the earlier studies (Batstone and Keller, 2001).

3.3.2. The correlation between EPS gel stiffness and granule's mechanical strength

The linear correlation between EPS gel stiffness (G^*), granule's shear strength ($S_{granule}$), and granule's resistance to compression ($E_{granule}$) is shown in Fig. 6**-c** and Fig. 6**-d**. In all cases a strong positive impact of EPS hydrogel stiffness on physical properties of granules can be seen ($r > 0.60$). Hence, this is the first study in anaerobic granular sludge field that clearly demonstrates how the EPS hydrogel stiffness affects the strength of granules. It must be noted that such trends are remarkable given a number of other factors, such as granule porosity, preciptates of carbonates, and microbe clustering denisty amongst others, which could also affect the physical properties of granules (Ding et al., 2015).

3.3.3. The correlation between EPS gel softening rate and granule's mechanical strength

In our study, granules with a higher shear strength (e.g. SD, KW, and P) contained EPS that formed hydrogels with lower softening rates ($\kappa < 0.9$) (Fig. 6**-e**). The softening rate of a hydrogel is frequently used to describe gel strength in other fields of application (e.g. biochemistry) (Jeon et al., 2022). However, it has not been reported as a property of EPS gels that could lend strength to granules (Seviour et al., 2009b).

When comparing all the samples, the softening rate of most EPS hydrogels showed strong correlation with granule's resistance to shear stress ($r = -0.85$, $p = 0.008$) (Fig. 6**-e**). One exception was the EPS gel formed from granules grown on soft drink wastewater (SD), which exhibited a higher Strain II (40 %) during the amplitude sweep (Table 3). The higher Strain II can lead to a delay at which strain the gel started to break. In general, the behaviour of EPS in the non-linear viscoelastic region seems to be crucial in determining the shear strength of anaerobic granules. This is logical considering the breakage of polymer networks upon exposure to shear. In contrast, no clear relationship can be found between granule's compression strength and EPS gel softening rate (Fig. 6**-f)**. To date investigations between granule's characterises and EPS viscoelastic properties mostly focused on LVE regime (Pagliaccia et al., 2022; Schambeck et al., 2020). Our findings suggest that the EPS hydrogel softening rate at non-linear regime could be a key parameter to explain granule's shear strength.

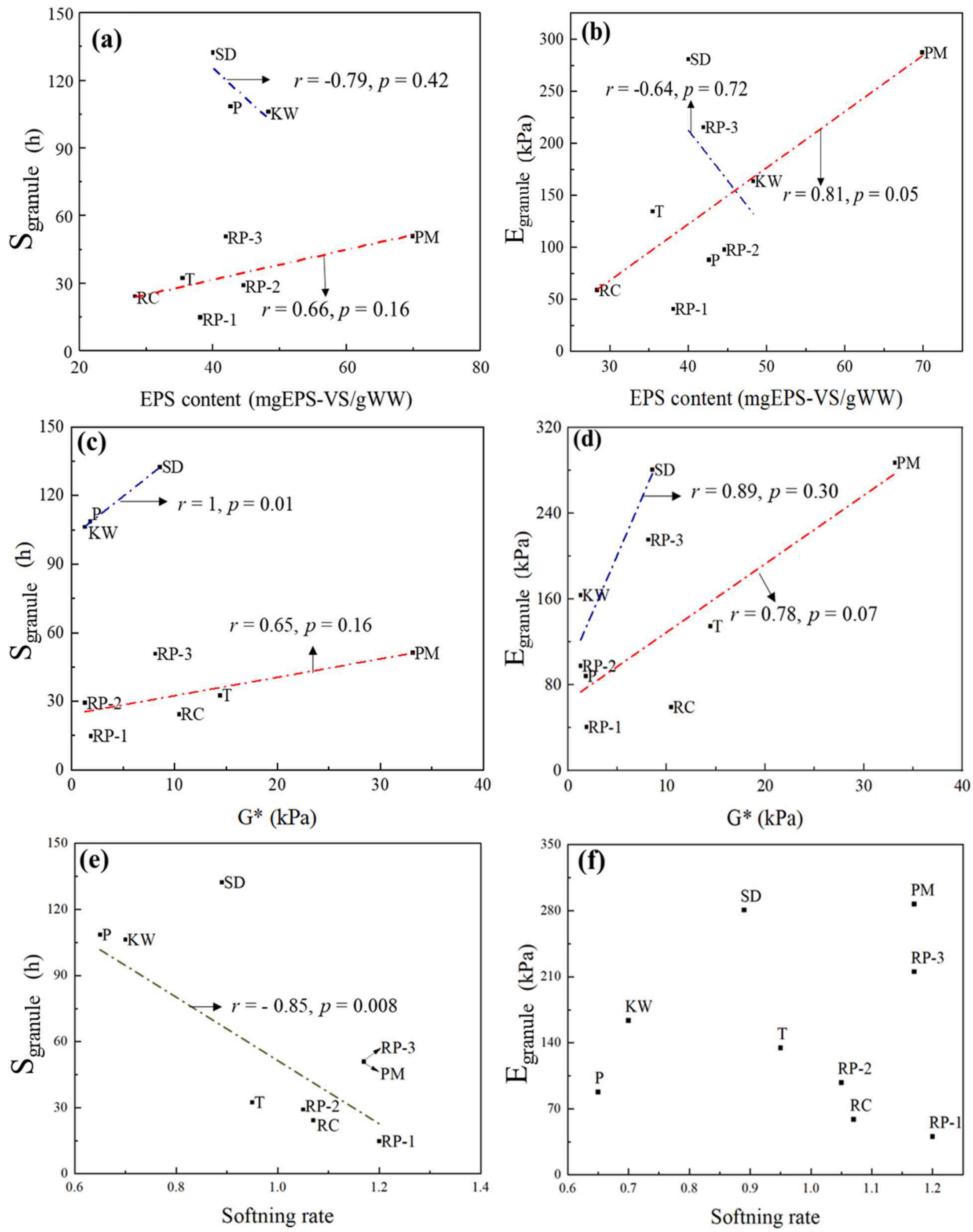

Fig. 6. Relationship between (a) granule's shear strength ($S_{granule}$) and EPS content; (b) granule's resistance to compression ($E_{granule}$) and EPS content; (c) granule's shear strength ($S_{granule}$) and EPS gel stiffness (G*); (d) granule's resistance to compression ($E_{granule}$) and EPS gel stiffness (G*). The blue dashed lines represent the trend lines for data points SD, KW, and P; the red dashed lines represent the trend lines for the remaining data. Relationship between (e) granule's shear strength ($S_{granule}$) and EPS gel softening rate (κ); (f) granule's resistance to compression ($E_{granule}$) and EPS gel softening rate (κ). The green dashed line represents the trend line for the data points, except SD. PM-papermill, P-potato, RP-recycled paper, SD-soft drink, KW-kitchen waste, RC- rendering condensate, and T-tannery.

4. Conclusions

In this study, we present solid evidence that EPS determine the physical properties of anaerobic granules to a large extent and introduce a new parameter, softening rate, to be evaluated when studying EPS gel strength. With the clear indications of this work, future studies should be taken up to include more various granules in light of the statistical significance of the results. An interesting outcome seems that, in anaerobic granules the protein fraction is contributing more to the granule's shear strength compared to the aerobic counterpart. This certainly warrants further investigations on the role of proteins in anaerobic granule EPS.

CRediT authorship contribution statement

Chang Gao: Data curation, Formal analysis, Writing – original draft. **Mehdi Habibi:** Supervision, Writing – review & editing. **Tim L.G. Hendrickx:** Writing – review & editing. **Huub H.M. Rijnaarts:**

Supervision, Writing – review & editing. **Hardy Temmink:** Conceptualization, Investigation. **Dainis Sudmalis:** Conceptualization, Formal analysis, Investigation, Writing – review & editing, Supervision.

Declaration of competing interest

The authors declare that they have no known competing financial interests or personal relationships that could have appeared to influence the work reported in this paper.

Data availability

Data will be made available accordong to WUR's research data policy.

Acknowledgments

This research was financially supported by the Chinese Scholarship Council and Paques Technology B.V.. The authors would like to thank Waterstromen for the sampling of granules and for providing the parameters of WWTPs' operation.

Appendix A. Supplementary data

Supplementary data to this article can be found online at https://doi.org/10.1016/j.biortech.2024.131233.

References

Amrhein, V., Greenland, S., McShane, B., 2019. Retire statistical significance. https://www.nature.com/articles/d41586-019-00857-9.
APHA, 1999. Standard Methods for the Examination of Water and Wastewater. American Public Health Association, Washington DC.
Ayol, A., Dentel, S.K., Filibeli, A., 2006. Toward efficient sludge processing using novel rheological parameters: dynamic rheological testing. Water Sci. Technol. 54, 17–22. https://doi.org/10.2166/wst.2006.542.
Batstone, D.J., Keller, J., 2001. Variation of bulk properties of anaerobic granules with wastewater type. Water Res. 35 (7), 1723–1729. https://doi.org/10.1016/S0043-1354(00)00446-2.
Campo, R., Carretti, E., Lubello, C., Lotti, T., 2022. Recovery of structural extracellular polymeric substances (seps) from aerobic granular sludge: insights on biopolymers characterization and hydrogel properties for potential applications. J. Environ. Manage. 324, 116247. https://doi.org/10.1016/j.jenvman.2022.116247.
D'Abzac, P., Bordas, F., Van Hullebusch, E., Lens, P.N., Guibaud, G., 2010. Extraction of extracellular polymeric substances (EPS) from anaerobic granular sludges: comparison of chemical and physical extraction protocols. Appl Microbiol Biotechnol. 85, 1589–1599. https://doi.org/10.1007/s00253-009-2288-x.
de Graaff, D.R., van Dijk, E.J.H., van Loosdrecht, M.C.M., Pronk, M., 2020. Strength characterization of full-scale aerobic granular sludge. Environ. Technol. 41 (13), 1637–1647. https://doi.org/10.1080/09593330.2018.1543357.
DeBenedictis, E.P., Keten, S., 2019. Mechanical unfolding of alpha- and beta-helical protein motifs. Soft Matter 15, 1243–1252. https://doi.org/10.1039/C8SM02046A.
Ding, Z., Bourven, I., Guibaud, G., van Hullebusch, E.D., Panico, A., Pirozzi, F., Esposito, G., 2015. Role of extracellular polymeric substances (EPS) production in bioaggregation: application to wastewater treatment. Appl. Microbiol. Biotechnol. 99 (23), 9883–9905. https://doi.org/10.1007/s00253-015-6964-8.
Dubé, C.-D., Guiot, S.R., 2019. Characterization of the protein fraction of the extracellular polymeric substances of three anaerobic granular sludges. AMB Express 9 (1), 1–11. https://doi.org/10.1186/s13568-019-0746-0.
DuBois, M., Gilles, K.A., Hamilton, J.K., Rebers, P.A., Smith, F., 1956. Colorimetric method for determination of sugars and related substances. Anal. Chem. 28 (3), 350–356. https://doi.org/10.1021/ac60111a017.
Farno, E., Baudez, J.C., Parthasarathy, R., Eshtiaghi, N., 2016. The viscoelastic characterisation of thermally-treated waste activated sludge. Chem. Eng. J. 304, 362–368. https://doi.org/10.1016/j.cej.2016.06.082.
Felz, S., Al-Zuhairy, S., Aarstad, O.A., van Loosdrecht, M.C.M., Lin, Y.M., 2016. Extraction of structural extracellular polymeric substances from aerobic granular sludge. J. Visual. Experiment. JOVE 115, 54534. https://doi.org/10.3791/54534.
Felz, S., Kleikamp, H., Zlopasa, J., van Loosdrecht, M.C.M., Lin, Y., 2020. Impact of metal ions on structural EPS hydrogels from aerobic granular sludge. Biofilm 2, 100011. https://doi.org/10.1016/j.bioflm.2019.100011.
Flemming, H.-C., Wingender, J., 2010. The biofilm matrix. Nat. Rev. Microbiol. 8, 623–633. https://doi.org/10.1038/nrmicro2415.
Forster, C.F., Quarmby, J., 1995. The physical characteristics of anaerobic granular sludges in relation to their internal architecture. Antonie Van Leeuwenhoek 67, 103–110. https://doi.org/10.1007/BF00872198.
Gagliano, M.C., Sudmalis, D., Pei, R., Temmink, H., Plugge, C.M., 2020. Microbial community drivers in anaerobic granulation at high salinity. Front. Microbiol. 11, 235. https://doi.org/10.3389/fmicb.2020.00235.
Giménez-Ribes, G., Yang, J., He, Q., Habibi, M., Sagis, L.M.C., 2023. Self-similarity and Payne effect of whey protein-escin mixtures at the air-water interface. Food Hydrocoll. 139, 108554 https://doi.org/10.1016/j.foodhyd.2023.108554.
Guo, H., Felz, S., Lin, Y., Van Lier, J.B., De Kreuk, M., 2020. Structural extracellular polymeric substances determine the difference in digestibility between waste activated sludge and aerobic granules. Water Res. 181, 115924 https://doi.org/10.1016/j.watres.2020.115924.
Horan, N.J., Yaser, A.Z., Wid, N. (Eds.), 2018. Anaerobic Digestion Processes: Applications And Effluent Treatment (Ser. Green energy and technology). Springer, 10.1007/978-981-10-8129-3.
Hudayah, N., Suraraksa, B., Chaiprasert, P., 2019. Impact of eps and chitosan combination on enhancement of anaerobic granule quality during simultaneous microbial adaptation and granulation. J. Chem. Technol. Biotechnol. 94 (11), 3725–3735. https://doi.org/10.1002/jctb.6180.
Jaishankar, A., McKinley, G.H., 2013. Power-law rheology in the bulk and at the interface: quasi-properties and fractional constitutive equations. Proceedings: Mathematical. Phys. Eng. Sci. 469 (2149), 1–18. https://doi.org/10.1098/rspa.2012.0284.
Javanmardi, Y., Colin-York, H., Szita, N., Fritzsche, M., Moeendarbary, E., 2021. Quantifying cell-generated forces: poisson's ratio matters. Commun. Phys. 4, 237. https://doi.org/10.1038/s42005-021-00740-y.
Jeon, O., Kim, T.-H., Alsberg, E., 2022. Reversible dynamic mechanics of hydrogels for regulation of cellular behavior. Acta Biomater. 136, 88–98. https://doi.org/10.1016/j.actbio.2021.09.032.
Lee, D.-J., Chen, Y.-Y., Show, K.-Y., Whiteley, C.G., Tay, J.-H., 2010. Advances in aerobic granule formation and granule stability in the course of storage and reactor operation. Biotechnol. Adv. 28, 919–934. https://doi.org/10.1016/j.biotechadv.2010.08.007.
Li, Z., Lin, L., Liu, X., Wan, C., Lee, D.-J., 2020. Understanding the role of extracellular polymeric substances in the rheological properties of aerobic granular sludge. Sci. Total Environ. 705 https://doi.org/10.1016/j.scitotenv.2019.135948.
Lier, J.B., 2015. Celebrating 40 years anaerobic sludge bed reactors for industrial wastewater treatment. Rev Environ Sci Biotechnol. https://doi.org/10.1007/s11157-015-9375-5.
Lin, Y.M., Wang, L., Chi, Z.M., Liu, X.Y., 2008. Bacterial alginate role in aerobic granular bio-particles formation and settleability improvement. Sep. Sci. Technol. 43, 1642–1652. https://doi.org/10.1080/01496390801973805.
Liu, H., 2021. Chapter 7 - Description methods of spatial wind along railways. In: Liu, H. (Ed.), Wind Forecasting in Railway Engineering. Elsevier, pp. 251–282 https://doi.org/10.1016/B978-0-12-823706-9.00007-7.
Liu, Y., Tay, J.-H., 2002. The essential role of hydrodynamic shear force in the formation of biofilm and granular sludge. Water Res. 36 (7), 1653–1665. https://doi.org/10.1016/s0043-1354(01)00379-7.
Ma, Y.-J., Xia, C.-W., Yang, H.-Y., Zeng, R.J., 2014. A rheological approach to analyze aerobic granular sludge. Water Res. 50, 171–178. https://doi.org/10.1016/j.watres.2013.11.049.
McHugh, S., O'Reilly, C., Mahony, T., Colleran, E., O'Flaherty, V., 2003. Anaerobic granular sludge bioreactor technology. Rev. Environ. Sci. Biotechnol. 2 (2–4), 225–245. https://doi.org/10.1023/B:RESB.0000040465.45300.97.
Ni, S.Q., Sun, N., Yang, H., Zhang, J., Ngo, H.H., 2015. Distribution of extracellular polymeric substances in anammox granules and their important roles during anammox granulation. Biochem. Eng. J. 101, 126–133. https://doi.org/10.1016/j.bej.2015.05.014.
Pagliaccia, B., Durieux, S., Bessiere, Y., Bounouba, M., Sarkis, A.B., Girbal-Neuhauser, E., Carretti, E., Lubello, C., Lotti, T., Paul, E., 2022. Insights on the hydrogel-forming ability and post-gelling mechanical properties of structural extracellular polymeric substances (sEPS) from aerobic granular sludge (AGS): A comparison with model biopolymers. J. Water Process Eng. 49, 103076 https://doi.org/10.1016/j.jwpe.2022.103076.
Pereboom, J.H.F., 1997. Strength characterisation of microbial granules. Water Sci. Technol. J. Int. Assoc. Water Pollut. Res. 36 (6/7), 141. https://doi.org/10.1016/S0273-1223(97)00517-9.
Quarmby, J., Forster, C.F., 1995. An examination of the structure of UASB granules. Water Res. 29 (11), 2449–2454. https://doi.org/10.1016/0043-1354(95)00083-W.
Sarkis, A.B., 2023. Characterization of exopolymers from aerobic granules: towards their valorization as bio-sourced materials issued from the treatment of effluents. Bacteriology. Université Paul Sabatier Toulouse III 2023. https://theses.hal.science/tel-04277118.
Schambeck, C.M., Girbal-Neuhauser, E., Böni, L., Fischer, P., Bessière, Y., Paul, E., da Costa, R.H.R., Derlon, N., 2020. Chemical and physical properties of alginate-like EPSs of aerobic granules and flocs produced from different wastewaters. Bioresour. Technol. 312, 123632 https://doi.org/10.1016/j.biortech.2020.123632.
Seviour, T., Pijuan, M., Nicholson, T., Keller, J., Yuan, Z., 2009a. Gel-forming exopolysaccharides explain basic differences between structures of aerobic sludge granules and floccular sludges. Water Res. 43, 4469–4478. https://doi.org/10.1016/j.watres.2009.07.018.
Seviour, T., Pijuan, M., Nicholson, T., Keller, J., Yuan, Z., 2009b. Understanding the properties of aerobic sludge granules as hydrogels. Biotechnol. Bioeng. 102, 1483–1493. https://doi.org/10.1002/bit.22164.
Sheng, G.-P., Yu, H.-Q., Li, X.-Y., 2010. Extracellular polymeric substances (EPS) of microbial aggregates in biological wastewater treatment systems: A review. Biotechnol. Adv. 28, 882–894. https://doi.org/10.1016/j.biotechadv.2010.08.001.

Shi, Y., Liu, Y., 2021. Evolution of extracellular polymeric substances (EPS) in aerobic sludge granulation: Composition, adherence and viscoelastic properties. Chemosphere 262, 128033. https://doi.org/10.1016/j.chemosphere.2020.128033.

Thapa, P., 2019. Effects of granulation process variables on the physical properties of dosage forms by combination of experimental design and principal component analysis. Asian J. Pharm. Sci. 14 (3), 287–304. https://doi.org/10.1016/j.ajps.2018.08.006.

van Lier, J.B., 2008. High-rate anaerobic wastewater treatment: diversifying from end-of-the-pipe treatment to resource-oriented conversion techniques. Water Sci. Technol. J. Int. Assoc. Water Pollut. Res. 57 (8), 1137–1148. https://doi.org/10.2166/wst.2008.040.

Wang, S., Huang, X., Liu, L., Shen, Y., Yan, P., Chen, Y., Guo, J., Fang, F., 2020. Understanding the mechanism in aggregation ability between aerobic and anammox granular sludge from the perspective of exopolysaccharides. J. Water Process Eng. 38, 101629 https://doi.org/10.1016/j.jwpe.2020.101629.

Wang, Z.-W., Liu, Y., Tay, J.-H., 2005. Distribution of EPS and cell surface hydrophobicity in aerobic granules. Appl Microbiol Biotechnol 69, 469–473. https://doi.org/10.1007/s00253-005-1991-5.

Williams, K., Percival, F., Merino, J., Mooney, H., 1987. Estimation of tissue construction cost from heat of combustion and organic nitrogen content. Plant Cell Environ. 10 (9), 725–734. https://doi.org/10.1111/1365-3040.ep11604754.

Willits, R.K., Skornia, S.L., 2004. Effect of collagen gel stiffness on neurite extension. J. Biomater. Sci. Polym. Ed. 15 (12), 1521–1531. https://doi.org/10.1163/1568562042459698.

Zayas, J.F., 1997. Gelling properties of proteins. In: Functionality of Proteins in Food. Springer, Berlin Heidelberg, Berlin, Heidelberg, pp. 310–366, 10.1007/978-3-642-59116-7_7.

Zhao, S.-S., Gan, P., Lu, L.-H., Chen, Y.-L., Zhou, Y.-F., Wang, S.-F., Wang, Z.-W., Zhang, J., 2022. Deciphering the formation of sludge blanket structure in anaerobic granular systems from the perspective of bubble-entrapment assumption. Chem. Eng. J. 428 https://doi.org/10.1016/j.cej.2021.131324.